Adsorption of a wide variety of antibiotics on graphene-based nanomaterials: a modelling study

Matej Kern, Sanja Škulj, Marko Rožman*

Ruđer Bošković Institute, Bijenička cesta 54, 10000 Zagreb, Croatia

*Corresponding author.

Email addresses:

Matej Kern: matej.kern@irb.hr

Sanja Škulj: sanja.skulj@irb.hr

Marko Rožman: marko.rozman@irb.hr

Abstract

The knowledge on the sorption behaviour of antibiotics on nanomaterials is limited, especially regarding the reaction mechanism on the surface of carbon nanomaterials, which may determine both the adsorptive capacity and regeneration efficiency of graphene adsorbers. In this work, we used molecular modelling to generate the most comprehensive (to date) adsorption dataset for pristine and functionalised graphene interacting with 8 β-lactams, 3 macrolide, 12 quinolone, 4 tetracycline, 15 sulphonamide, trimethoprim, 2 lincosamide, 2 phenicole and 4 nitroimidazole antibiotics, and their transformation products in water and *n*-octanol. Results show that various non-covalent interactions that operate simultaneously, including van der Walls dispersion forces, π-interactions, hydrophobic interaction and hydrogen bonding, facilitate adsorption. The molecular properties of antibiotics and graphene/graphene oxide, as well as the composition of the background solution regulate the magnitude of these interactions. Our findings demonstrate that the most efficient method for the removal of antibiotics from aquatic environments is the use of graphene at environmental pH. The subsequent regeneration of the sorbent is best achieved through washing with slightly basic (pH 8-10) non-polar solvents. The obtained theoretical insights expand and complement experimental observations and provide important information that can contribute to further exploration into the adsorbent properties of graphene-based materials, and towards the development of predictive adsorption models.

Keywords: pharmaceuticals, density functional theory, nanomaterials, adsorption, water and wastewater treatment.

Introduction

The omnipresence of both narrow and broad-spectrum antibiotics in the environment around the world is a well-established fact. Accordingly, a large number of studies have reported on the occurrence of antibiotics in natural and engineered aquatic environments(Kovalakova et al., 2020; Kümmerer, 2009). The continued pressure of antibiotics on aquatic environments has resulted in alterations of bacterial community composition, the emergence of antibiotic resistant bacteria, and their uptake by aquatic plants and animals(Previšić et al., 2021; Rizzo et al., 2013; van der Grinten et al., 2010; Wang et al., 2020). The presence of broad-spectrum antibiotics is currently recognized as a very serious public health concern due to the disappearance of some microbial populations and their ecological functioning, as well as risks associated with antibiotic resistome, toxic effects on higher trophic level organisms and the transport of antibiotics to terrestrial ecosystems(Previšić et al., 2021; Rizzo et al., 2013; van der Grinten et al., 2010; Wang et al., 2020). This has spurred research on many processes that may be applied for the remediation of antibiotics from natural and engineered aquatic environments, as the issue is expected to grow in importance with time (Phoon et al., 2020).

The processes explored for the removal of antibiotic contaminants include adsorption(Sophia et al., 2016), advanced oxidation processes(Thakur and Kandasubramanian, 2019), biodegradation(Baselga-Cervera et al., 2019), membrane filtration(Wang et al., 2016) and reverse osmosis(Albergamo et al., 2019). Of these, adsorption offers a simple and easily implementable method for (waste)water treatment. Carbon nano-materials (CNMs), such as graphene and graphene oxide, have emerged as efficient adsorbents for the remediation of (waste)waters (Ersan et al., 2017; Sophia et al., 2016). Also, the presence of an efficient nano-sorbent was shown to greatly benefit other wastewater treatment processes such as persulphate-based oxidation (Zhou et al., 2020) and photocatalysis (Rahnama et al., 2021). Consequently, the exploration of graphene-based materials as next-generation adsorbents for

71 the treatment of waters and wastewaters impacted by antibiotics has been intensified in recent
72 years.

73 The use of graphene-based materials for the adsorption of various antibiotics has been
74 reported in literature(Ersan et al., 2017; Yu et al., 2016). Experimental studies have reported
75 on the kinetics and thermodynamics of the adsorption of some members of tetracycline (Gao
76 et al., 2012; Lin et al., 2013; Rostamian and Behnejad, 2018), quinolone (Zhu et al., 2015),
77 and the sulphonamide(Chen et al., 2015; Rostamian and Behnejad, 2016) family onto CNMs.
78 Studies agree that graphene-based materials exhibit a large adsorption capacity towards the
79 studied antibiotics. In addition to the intrinsic properties of the adsorbent in use, most of the
80 studies agree on the significant effect of solution pH, ionic strength and temperature on the
81 adsorption of antibiotics. Adsorption interactions are categorized as physisorption caused by
82 the non-covalent interactions between antibiotics and graphene-based materials. However, the
83 actual nature of non-covalent interactions, i.e. electrostatic, hydrogen bonds, hydrophobic,
84 Van der Waals (vdW) or π interactions and their relative contributions is widely speculated.
85 The contribution of hydrophobic interactions, explored through adsorption in different
86 solvents e.g. n-octanol, has also received little attention given their importance in adsorbent
87 regeneration and possible adsorbate transport effects. Several recent reviews on this topic
88 have emphasized that "a clear understanding of the reaction mechanism on the surface of
89 carbon nanomaterials is crucial to the design of carbon adsorbers since these reactions may
90 determine both the adsorptive capacity and regeneration efficiency of carbon adsorbers and
91 ultimately their economic viability"(Ersan et al., 2017; Sophia et al., 2016; Yu et al., 2016).

92 Although scarce, computational approaches have been shown to facilitate understanding of
93 the fundamental mechanism regarding the adsorption of some aromatic compounds and
94 pharmaceutically active compounds on the surface of carbon nanomaterials(Ai et al., 2019;
95 Alammar et al., 2020; He et al., 2018; Ivanković et al., 2021; Jauris et al., 2016; Song et al.,

2016; Tang et al., 2020; Zhang et al., 2016). In addition to providing a fundamental understanding of adsorption on these materials, computational approaches may reveal the influence of the level of graphene-based materials oxidation, solution pH and solvent polarity to the overall adsorption(Ivanković et al., 2021). These approaches also enable us to use models of graphene oxide with a consistent degree of oxidation which has been difficult to achieve experimentally since slight modifications to the commonly used Hummers' method lead to differences in both degree of oxidation and adsorption properties of the resultant nanomaterial(Kang et al., 2016; Luo et al., 2015; Morimoto et al., 2017; Yadav and Lochab, 2019).

The aim of this work is to fill the current knowledge gap and provide a molecular level details of the adsorption of 51 antibiotics (most of them not studied so far) on graphene and graphene oxide in water and *n*-octanol following our earlier uniform and adequate theoretical framework used for modeling the adsorption of pharmaceutically active compounds (not antibiotics) on several CNMs(Ivanković et al., 2021). Adsorption process is broken down by antibiotic classes allowing integrated comparison of the antibiotic compounds with significantly different physico-chemical properties. In addition, we aim to contribute to the enlargement of the graphene based nanomaterials adsorption database for sorbent/sorbate systems for which experimental data is either difficult or enduring to acquire. Obtained results are expected to assist in the "tuning" of the adsorption of antibiotics on graphene-based materials, and to help with risk assessment and pollution control of both graphene-based materials and antibiotics.

Materials and methods

Selection of antibiotics

Several hundred different antibiotic substances are used in human and veterinary medicine (Kovalakova et al., 2020; Kümmerer, 2009). Recent overviews of antibiotic use have shown that in the European region the most prescribed antibiotics correspond to the β-lactam, macrolide, quinolone, tetracycline, sulphonamide (including trimethoprim) and lincosamide classes(Adriaenssens et al., 2011; Brauer et al., 2016; Versporten et al., 2014). In the European Union as well as in the United States, 50% of all antibiotics prescribed annually are used in human medicine, while the other 50% have applications in veterinary medicine, agriculture and aquaculture (Kovalakova et al., 2020; Kümmerer, 2009). In addition to the aforementioned classes, phenicole and nitroimidazole class antibiotics are extensively used for food-producing animals. Although their use has been restricted in many locations, the residues of these antibiotics continue to be detected in food items and the environment (Hassan et al., 2013; Kümmerer, 2009). Taking into consideration the data on their use and occurrence in water and wastewater environments, we selected a representative dataset of 8 β-lactams, 3 macrolides, 12 quinolones, 4 tetracyclines, 15 sulphonamides, trimethoprim, 2 lincosamides, 2 phenicole and 4 nitroimidazoles. The selected antibiotics and their properties are listed in table S1 Supplementary information (SI).

Model building

Models of the selected antibiotics and nanomaterials were built using GausView 6.0 software(Dennington, Roy; Keith, Todd A.; Millam, 2016). Geometry optimizations were then performed at the B3LYP-D3 / 6-31 G(d) level of theory in water (ε = 78.3553) and *n*-octanol (ε = 9.8629) using the SMD implicit solvation model at 298 K and 1 bar(Becke, 1993;

142 Grimme et al., 2010; Marenich et al., 2009; Stephens et al., 1994). Harmonic frequency
143 analysis was done to confirm that the obtained structures were minima on the potential energy
144 surface. Protons were added or removed from the antibiotic models as was required to
145 simulate different solution pH based on the functional groups and pK_a of the antibiotic, listed
146 in table S2.

147 Graphene and graphene oxide sheets were represented by models of varying sizes that contain
148 from 54 to 144 and from 54 to 140 carbon atoms, respectively. Passivation of model edges
149 was achieved by the addition of hydrogen atoms. Graphene oxide models contain hydroxyl
150 and epoxide functional groups, but not carboxyl functional groups, as is appropriate for a low
151 degree of oxidation(Morimoto et al., 2016). Models of graphene oxide were not adjusted for
152 pH because, while they are representative at acidic and neutral pH, the removal of protons
153 required to model graphene oxide at pH > 9.8 results(Konkena and Vasudevan, 2012) in great
154 difficulties with the convergence of the SCF procedure that is an integral part of the
155 calculation of model energies, therefore pH ranges considered in this work stop at pH 10.
156 Other approaches to obtaining SCF convergence such as quadratic convergence procedures,
157 while possible, incur an unfeasibly large computational cost given the size and number of the
158 adsorption complexes studied. Nanomaterial models of different sizes were constructed to
159 decrease the computational cost of adsorption complexes constructed with smaller antibiotic
160 models where little benefit to accuracy would be achieved through the use of large
161 nanomaterial models. The size effect of graphene models introduced by this approach was
162 shown to have negligible impact on calculated binding energies.(Daggag et al., 2019)

163

Adsorption Complexes

Models of adsorption complexes were generated using a three-step process following the procedure described in our previous publication(Ivanković et al., 2021). Briefly, antibiotic models were placed above the center of an adequately-sized nanomaterial model in six possible orientations. Following this, all preliminary adsorption complexes were subject to geometry optimization by the PM6-D3H4 semi-empirical method with the use of the COSMO implicit solvation model as reasonable accuracy was shown to be achievable by this method(Sedlak et al., 2013). Of the six preliminary adsorption complexes, the most stable, in which no bonding or hydrogen transfers occurred, were used as input for further geometry optimizations at the B3LYP-D3 / 6-31 G(d) level of theory in water (ε = 78.3553) and *n*-octanol (ε = 9.8629) using the SMD implicit solvation model(Marenich et al., 2009). The final geometries were confirmed as minima by harmonic frequency analysis. The level of theory employed in this procedure represents an excellent trade-off between the accuracy and computational cost of describing dispersion dominated supramolecular complexes, as shown in comparison against the QCISD(T)/CBS method(Sedlak et al., 2013).

Computational details

Adsorption enthalpy (ΔH), which indicates the intensity of interaction between the antibiotic and CNM surface, was derived according to the following equation:

$$\Delta H = H_{\text{complex}} - H_{\text{antibiotic}} - H_{\text{CNM}} + BSSE$$

where H_{complex} is the enthalpy of the adsorption complex, $H_{\text{antibiotic}}$ is the enthalpy of the antibiotic, H_{CNM} is the enthalpy of CNM, and BSSE is the basis set superposition error correction. Counterpoise correction(Boys and Bernardi, 1970; Simon et al., 1996) was used to calculate the basis set superposition error and compensate for it. Gibbs free energy (ΔG) of

adsorption was calculated analogously to the adsorption enthalpy (ΔS), using the harmonic oscillator approximation, with the addition of the correction for the change from gas-phase at 1 atmosphere of pressure to liquid-phase at 1 M concentration. Iogansen's relationship(Iogansen, 1999) was used to calculate the enthalpies of the formation of hydrogen bonds from the redshift of donor – hydrogen stretching vibrations in cm^{-1}, which was possible only for hydrogen bonds - the formation of which resulted in a redshift larger than 40 cm^{-1}. Calculated hydrogen bond enthalpies of formation were summed for each adsorption complex:

$$\Delta H_{\mathrm{H-bond}} = \sqrt{1.92(\Delta\nu - 40)}$$

$$\Delta H_{\mathrm{H-bonds}} = \sum \Delta H_{\mathrm{H-bond}}$$

All semi-empirical calculations were performed using Mopac2016 software (MOPAC2016, James J. P. Stewart, Stewart Computational Chemistry, Colorado Springs, CO, USA), while DFT calculations were performed using Gaussian 16(Frisch et al., 2016).

Performance against experimental data

The comparison of computed vs. reference values of Gibbs free energy of adsorption, when available, is presented in Table S3 - SI. The data show a mean signed error of -0.79 kJ mol^{-1} and mean unsigned error of 7.90 kJ mol^{-1} which compares favourably with the performance of the SMD model in the solvation free energies at the B3LYP-D3 / 6-31 G(d) level of theory for ions in water(Marenich et al., 2009). At this point it should be noted that the used graphene and graphene oxide structures are single sheet of uniform size and have a homogeneous surface and strictly defined functional groups comparing to wrinkles, folds, vacancies and non-uniformly distributed functional groups of real life nanomaterials(Ersan et al., 2017).

Adsorption in real wastewater treatment systems is also influenced by effects such as ionic strength of the solution and competitive adsorption of other ions and molecules present in the solution. The study of these effects is a topic into itself and falls beyond the scope of this work even if they may account for possible discrepancies between experimental and theoretical values. However, the strong agreement with reference experimental data, in addition to the previous successful application of this model(Ivanković et al., 2021), verifies the ability of the model to reproduce experimental results adequately.

Results and discussion

Adsorption mechanism

The results of the adsorption energies suggest a strong adsorption affinity of both graphene and hydroxylated graphene for the antibiotics. The studied antibiotics are spontaneously adsorbed onto the studied materials as indicated by generally negative ΔG values (the computed thermodynamic parameters are listed in Table 1 and Table S4 - SI due to large amount of data provided). Negative ΔH and ΔS values indicate an exothermic nature of the adsorption associated with ordering. While antibiotics are indeed spontaneously adsorbed onto nano-materials, their affinities vary between different classes and individual compounds. The magnitude of adsorption depends on the interplay between several non-covalent interactions such as van der Waals, π-interactions, hydrogen bonding, Coulombic ionic and hydrophobic interactions. In this respect, the relationship between certain categories of non-covalent interactions and adsorption energy was analysed.

Table 1 Gibbs free energies (in kJ mol^{-1}) of adsorption of antibiotics at pH 7 and 298 K.

Antibiotic	$\Delta G_{graphene}$	$\Delta G_{graphene\ oxide}$	$\Delta G_{graphene}$	$\Delta G_{graphene\ oxide}$
	water		*n*-octanol	
Macrolides				
Azithromycin	-77.5	-55.2	-84.2	-135.9
Clarithromycin	-78.3	-6.3	-43.0	-31.4
Erythromycin	-75.5	15.6	-58.3	-38.0
β-lactams				
Cefalexin	1.4	6.6	11.4	-2.8
Oxacillin	-33.6	1.9	16.5	13.8
Penicillin G	-24.9	-26.2	0.0	-11.8
Amoxicillin	1.0	-5.2	18.6	-25.1
Ampicillin	-14.5	-24.1	2.1	-45.2
Cefuroxime	-48.2	-42.2	-12.0	-48.1

Cloxacillin	-39.2	-25.9	-13.2	31.7
Dicloxacillin	-9.8	2.0	-4.7	15.7
Quinolones				
Ciprofloxacin	-40.7	-6.6	-1.0	-23.3
Flumequine	-7.0	-5.7	19.6	-0.3
Marbofloxacin	-8.7	-11.0	-4.7	-45.9
Nalidixic acid	-33.7	-31.6	-16.4	-29.8
Norfloxacin	-30.5	111.6	0.2	-2.2
Ofloxacin	-34.5	-19.1	-9.6	-1.9
Oxolinic acid	-22.4	5.8	4.0	-1.6
Pipemidic acid	-36.6	-22.1	0.2	-17.1
Enrofloxacin	-47.4	-13.8	-21.0	-27.0
Enoxacin	-36.4	3.2	37.6	-10.1
Danofloxacin	-17.3	-4.5	-1.6	-51.4
Difloxacin	-48.5	-31.4	-17.3	27.2
Nitroimidazoles				
Dimetridazole	-3.4	13.9	10.3	19.8
Metronidazole	-10.7	10.5	9.4	15.2
Ronidazole	-7.8	6.5	3.5	1.3
Metronidazole-OH	-4.9	30.2	5.2	7.7
Phenicoles				
Florfenicol	-20.1	-11.0	-2.1	2.3
Chlorampenicol	-35.0	-21.8	-15.8	-23.0
Sulphonamides				
N(4)-acetyl sulfadiazine	-10.0	-12.8	20.0	1.1
N-acetyl sulfamethoxazole	-17.3	18.7	10.3	21.1
N-acetylsulfapyridine	-35.1	-10.9	-17.4	5.1
Sulfabenzamide	-10.9	-6.2	22.5	8.9
Sulfadiazine	7.8	-5.4	13.7	-2.5
Sulfadimetoxine	-11.0	-8.6	12.9	20.8
Sulfadimidin	-19.3	3.1	-1.1	27.0
Sulfamerazine	-15.0	17.6	-13.4	-27.7
Sulfamethizole	-1.3	10.2	19.9	-19.9
Sulfamethoxazole	-6.2	-4.1	20.5	-0.5
Sulfamethoxypyridazine	-13.5	-7.5	13.3	-1.9
Sulfaquinoxaline	-16.9	-16.8	14.6	17.5

Sulfasalazine	-74.3	-32.5	-52.3	-70.1
Sulfathiazole	-18.5	20.9	-5.5	-93.0
Sulfisoxazole	-2.9	10.3	11.0	22.2
Tetracyclines				
Oxytetracycline	-47.7	-29.2	-26.0	-11.3
Tetracycline	-41.0	-20.6	-23.0	-84.8
Chlorotetracycline	-56.5	-18.1	-23.8	-11.3
Doxycycline	-64.8	-14.9	-33.6	-39.0
Trimethoprim				
Trimethoprim	-24.0	-39.4	-18.4	-56.8
Lincosamides				
Lincomycin	-43.5	-13.9	-20.9	-12.8
Clindamycin	-31.9	-30.2	-8.1	3.2

van der Waals dispersion

Average molecular polarizability has been proven to be a convenient and straightforward approximation to assess the contribution of vdW dispersion interactions to the enthalpy of adsorption in the absence of computationally expensive energy decomposition analysis(Gowtham et al., 2008; Lata and Vikas, 2021). Here, Spearman correlation, the use of which is clearly demonstrated by T. D. Gauthier(Gauthier, 2001), was used to assess the contribution of vdW interactions to adsorption enthalpy. A moderate to strong correlation was detected in the case of graphene in water (r_s = -0.6, p < .05) while lower correlations were seen for graphene oxide in water (r_s = -0.36, p < .05). The reduced contributions of vdW interactions to the enthalpy of adsorption from graphene to graphene oxide were expected as the hydroxyl-containing functional groups of graphene oxide disrupt the sp^2-bonded hexagonal honeycomb structure of graphene and introduce the possibility of hydrogen bonding. As noted in our previous publication (Ivanković et al., 2021), oxygen functional groups introduce sp^3 carbons onto the surface of graphene which lower the isotropic

polarizability of the graphene oxide layer (in comparison with the pristine graphene layer). In addition, the presence of hydroxyl groups and the subsequent formation of intermolecular hydrogen bonds result in an increase in the average distance between graphene flake and antibiotics by 1.2 Å, causing van der Waals attraction forces to exponentially drop. It is interesting to note that antibiotics display a greater distance (by 0.5 Å) compared to the non-antibiotic pharmaceuticals used in our previous study (Ivanković et al., 2021). This can be attributed to the steric effect, since antibiotics are larger molecules and on average have more functional groups. In *n*-octanol, we note the lower contribution of overall vdW interactions to adsorption enthalpy for both graphene and graphene oxide (r_s = -0.45, p < .05, r_s = -0.26, p < .05, respectively) due to the lower polarizability of molecules in *n*-octanol and the increased contribution of hydrogen bonds, as shown later. When the correlation is done separately for differently charged antibiotic entities (data in Table S5 - SI), we note that neutral and anionic molecular entities exhibit a stronger correlation than cationic. This can be reasoned by the denser electron clouds of cations which are not so easily polarized compared to e.g. the electron clouds of negative ions that contain excess electrons. For graphene in water, however, the Spearman correlation coefficients for anionic entities are lower than those obtained for cationic entities. We believe that the culprit is a noisier anionic dataset, since linear regression of the same data gives a steeper slope for anions than for cations.

π interactions

Interactions between π systems of adsorbate and adsorbent molecules are commonly thought to play a major role in the overall binding mechanism of antibiotics and other pharmaceutically active molecules(Peng et al., 2016; Tang et al., 2018; Zhang et al., 2019). In recent work, we found that pharmaceutically active molecules containing two aromatic rings had a lower enthalpy of adsorption on graphene than those containing one aromatic ring;

however, no significant difference was found for adsorption on graphene oxide(Ivanković et al., 2021). To examine whether this is valid for the adsorption of neutral antibiotic molecules on graphene and graphene oxide, average enthalpies of adsorption were calculated for groups containing zero, one and two aromatic rings and compared successively by Welch's t-test, Fig. 1 (and Table S6 - SI). Although a trend of increasing adsorption complex stability with the increase in number of aromatic rings is visible on graphene, no group showed significantly different adsorption enthalpy than the one adjacent to it on both nanomaterials in both solvents. Although this result was unexpected at first, it was clarified by examining the conformations of adsorption complexes. The group of molecules containing no aromatic rings was mostly comprised of macrolide antibiotics which, due to their size, experienced strong vdW interactions with the flat surface of graphene. Antibiotic molecules containing one aromatic ring commonly achieved parallel stacking of that ring with graphene (Fig. S1 SI), whereas molecules containing two aromatic rings were unable to do so for both of the rings as the structure of the explored antibiotics does not enable them to assume the conformations necessary for both rings to be parallel to the nanomaterial surface, Fig. 2 a). On graphene oxide, although the percentage of carbon atoms not bonded to oxygen atoms was on average 74%, no single area of sufficient size for a phenyl fragment to stack neatly on top of it remained. This, in conjunction with the possibility of forming hydrogen bonds, led to conformations where even molecules with only one aromatic ring rarely achieved the close stacking necessary for strong π-π interactions Fig. 2 b). Altogether, this led to an important observation suggesting that for molecules similar in size and structure to those explored in this work, having more than one aromatic ring would not additionally contribute to their overall adsorption energy via π-π interactions.

In addition to π-π interactions, when charged antibiotics interact with graphene ion – π interactions emerge as an adsorption-enhancement mechanism. The differences in adsorption

enthalpies between cationic and uncharged antibiotic molecules on graphene were found to be 20 and 18 kJ mol^{-1} in both water and *n*-octanol, respectively. This result is in agreement with the intensity noted for the favourable interactions of cations such as NH_4^+ and benzene ring(Kim et al., 2003). On the other hand, negatively charged antibiotic molecules display a less stable adsorption than any other charge entity, resulting in a clear trend of adsorption stability ranging from cations > zwitterions ≈ uncharged molecules > anions for adsorption on graphene. It is interesting to note that for graphene oxide in water this trend changes to cations > zwitterions ≈ uncharged molecules ≈ anions as the greater strength of hydrogen bonds in anion complexes compensates the unfavourable anion – π interactions.

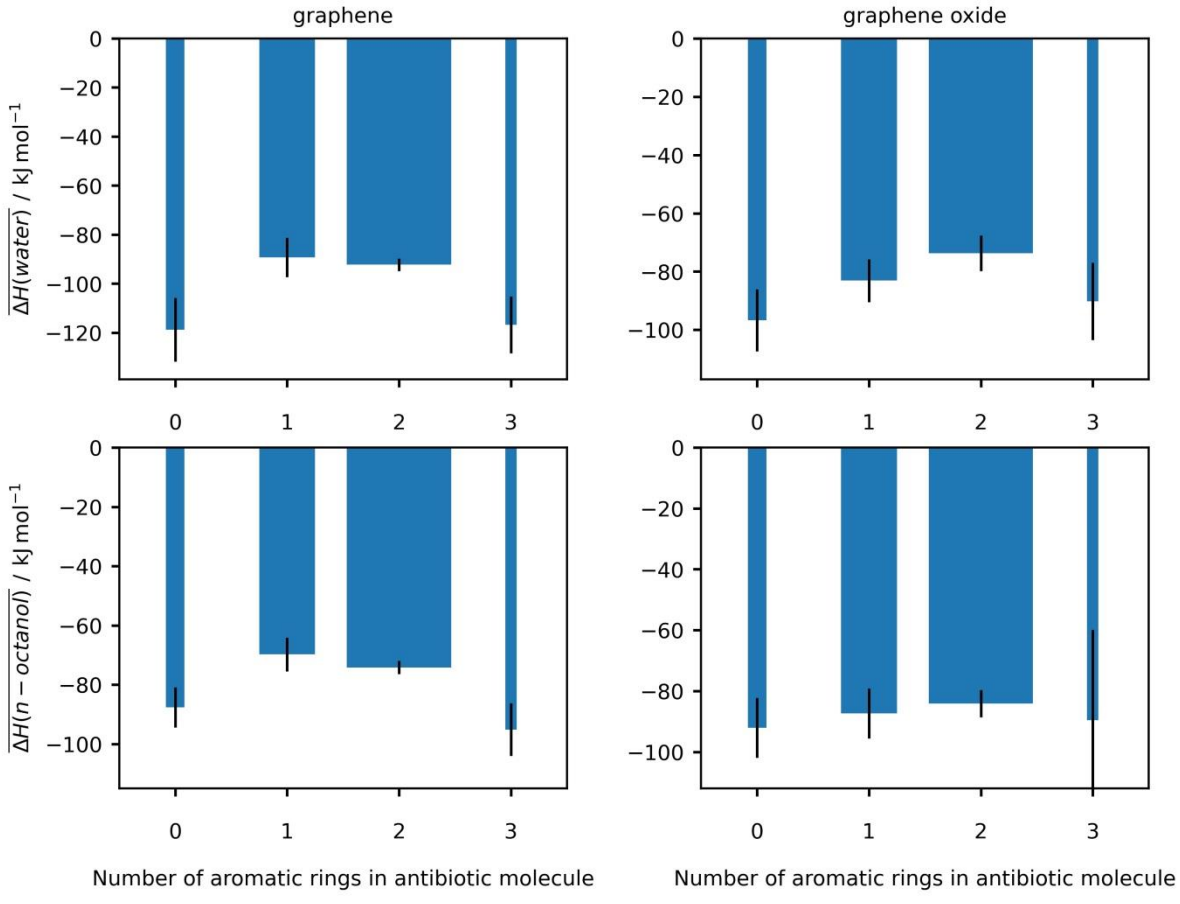

Fig. 1: Mean enthalpies of adsorption grouped by solvent, nanomaterial and number of the aromatic rings the antibiotic molecule contains. Bar thickness is adjusted to the number of contributing complexes.

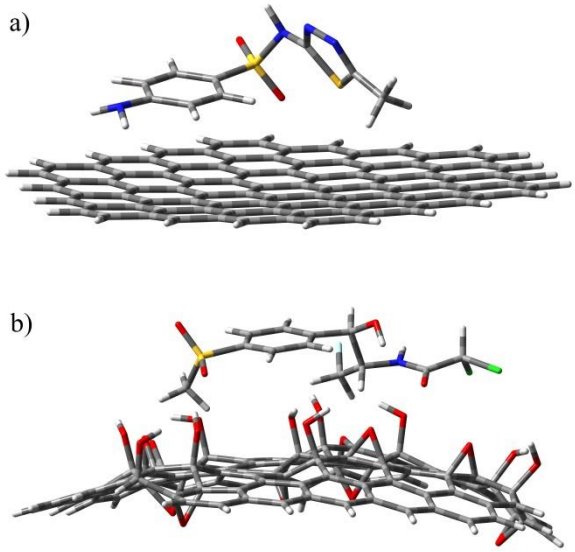

Fig. 2. Adsorption complexes on CNMs: a) Sulfamethizole adsorbed on graphene, unable to achieve parallel stacking of both rings. b) Florfenicol adsorbed on graphene oxide, unable to achieve close parallel stacking of its aromatic ring with the graphene oxide surface. Atoms are colored as using following color assignments: H - white, C - gray, N - blue, O - red, S - yellow, F- cyan and Cl - green. .

Hydrogen bonding

Hydrogen bonding has been shown to be an important contributing factor to the overall mechanism of adsorption in graphene sheets with high surface oxygen content(Ersan et al., 2017; Ivanković et al., 2021; Thakur and Kandasubramanian, 2019). Accordingly, we observe a very strong correlation (r_s = -1, p < .05) between the mean number of hydrogen bonds

formed in adsorbed complex and the mean adsorption ΔH. The latter suggests that antibiotic-graphene oxide complexes with a larger number of hydrogen bonds are more stable. The importance of hydrogen bonding is further corroborated through the considerable contribution of hydrogen bonds to the observed change in adsorption ΔH between graphene oxide and graphene (r_s = 0.42, p < .05). Significant correlations were found between all groups (except uncharged molecules) when the dependence between the sum of hydrogen bonds ΔH and the change in adsorption ΔH from pristine to graphene oxide is broken by charge. This finding is expected, as uncharged molecules adsorbed to graphene oxide are expected to have the highest contribution of vdW interactions to the total interaction energy due to having the largest correlation with polarizability.

Change in solvent polarity towards a lower dielectric constant (*n*-octanol) contributes on average 8 kJ mol^{-1} to complex stability, which is in line with the trend noted in previous studies on the effects of solvent polarity on hydrogen bonded systems(Aquino et al., 2002; Pašalić et al., 2010). The strengthening of hydrogen bonds is also suggested by the stronger contribution of hydrogen bond enthalpy of formation to the difference of adsorption enthalpy between graphene oxide and graphene (r_s = 0.59, p < .05). Broken by charge of the complex correlation is stronger or equal for all complexes except for cations where it is no longer significant. This result, along with the small contribution noted for vdW interactions, indicates that some other (most likely electrostatic) interaction contributes more substantially to the adsorption of antibiotic cations on graphene oxide in *n*-octanol.

Hydrophobic interactions

The antibiotics studied here, on average, form more stable adsorption complexes on graphene in water (Fig. 3) suggesting stronger complexation in more polar solvents. A moderate

correlation of Gibbs free energies of adsorption and the change in total solvent accessible surface area (r_s = 0.55, p < .05) indicates that the interaction between antibiotics and graphene is partly stronger due to the less solvated nonpolar surface of graphene. The obtained negative enthalpies and entropies of complexation (Table S3 – SI) invoke a nonclassical (enthalpic) hydrophobic effect(Kanagaraj et al., 2017). The same is true for the antibiotic–graphene oxide complexes formed in *n*-octanol, Fig. 3. This is in line with the lower hydrophobicity of graphene oxide(Konkena and Vasudevan, 2012) and further confirms the observed nonclassical hydrophobic, more generally solvophobic effect(Kanagaraj et al., 2017). These findings are consistent with reports on the increased complexation of pharmaceutically active compounds with pristine CNMs following the decreasing solubility of the CNMs (Ivanković et al., 2021).

When considering antibiotic molecules grouped by charge (Fig. 3), a more detailed pattern emerges. Although all groups form more stable adsorption complexes on graphene in water, the trend is not consistent on graphene oxide where cations and zwitterions form more stable complexes in *n*-octanol, while anions do so in water. The reason for this may be modulation of the hydrophobic effect by the electrostatic interactions. The low electric permittivity of *n*-octanol enhances both the favourable cation-π interactions and unfavourable anion-π interactions, alternating the range of complexation energy differences (Ivanković et al., 2021). The large differences observed in the behaviour of different antibiotics charge moieties adsorbed on graphene oxide, as solvent polarity changes, suggest an important issue that must be taken into account when considering methods of CNM regeneration.

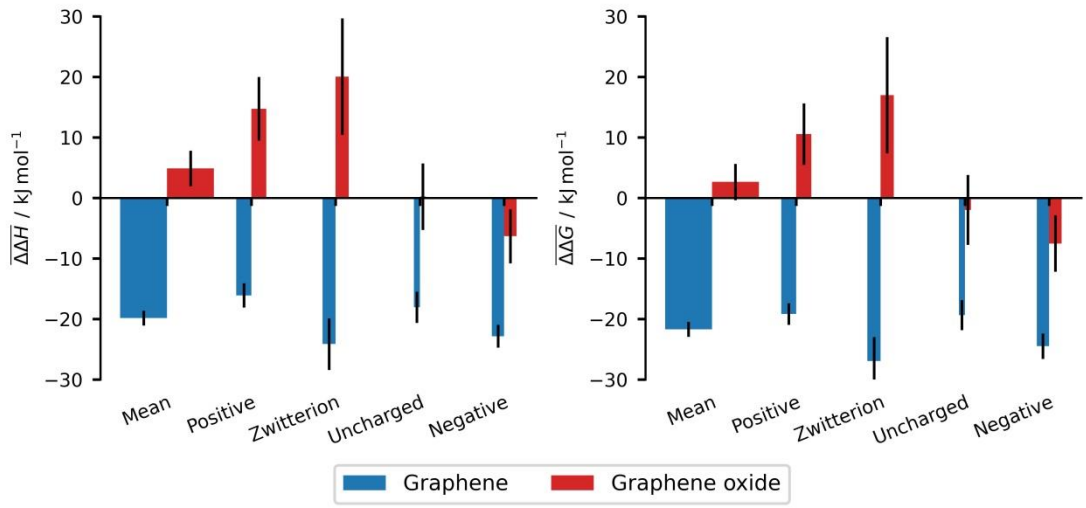

Fig. 3. Change of adsorption ΔH and ΔG from water to *n*-octanol ($\Delta\Delta H = \Delta H_{water} - \Delta H_{n\text{-octanol}}$, $\Delta\Delta G$ was calculated analogously). Overall mean $\Delta\Delta H$ and $\Delta\Delta G$ is presented, as well as mean values broken down by charge of a complex. Bar thickness is adjusted to the number of contributing complexes.

Differences in adsorption between classes of antibiotics

Macrolide antibiotics adsorb strongly on the examined nanomaterials, forming the most stable complexes on graphene in both water and *n*-octanol, Fig 4. This is expected due to their size, as they have (on average) double the mass and surface area compared to the rest of the analyzed ensemble. However, their size is penalized when they adsorb on graphene oxide, especially in water. The contributions of the adsorption ΔH on graphene oxide in water drop by 30%, which is most likely due to both a destabilizing solvophobic effect and the increase of over 1 Å in the distance between the centers of mass of the nanomaterial and antibiotic models, resulting in a large decrease of vdW interaction intensity.

Quinolones form stable adsorption complexes with both nanomaterials in both solvents at low pH, Fig. 4. In neutral conditions adsorption complexes are more stable on graphene than graphene oxide in water, which is consistent with previous findings by other researchers for ciprofloxacine(Rostamian and Behnejad, 2018; Zhu et al., 2015), whereas in *n*-octanol they are more stable on graphene oxide due to a solvophobic effect. The adsorption strength of quinolones on graphene follows the order: difloxacin ≈ enrofloxacine > ciprofloxacine > pipemidic acid ≈ enofloxacin ≈ ofloxacine ≈ nalidixic acid > norfloxacine > oxolinic acid > marbofloxacine ≈ flumequine (Table 1 and Table S3 SI). Correlation coefficients for adsorption ΔH versus isotropic polarizability (r_s = -0.4, p < .05) and the change in total solvent available surface area (r_s = -0.6, p < .05) indicate that their adsorption on graphene is governed by vdW interactions and the hydrophobic effect. This is corroborated by the lower correlation of adsorption ΔG with the change in total solvent accessible surface area in *n*-octanol (r_s = 0.4). Quinolones display a large drop in complex stability when switching solvent from water to *n*-octanol on graphene ($\Delta\Delta G$ > 25 kJ mol^{-1}) but an increase in complex stability ($\Delta\Delta G$ < -10 kJ mol^{-1}) for the same change on graphene oxide. This may be very useful for regeneration of the graphene with a low polarity solvent. On the other hand, one may experience difficulties with the desorption of quinolones from graphene oxide at neutral pH in low polarity solvents. The examination of other pH regions reveals that below pH 6 adsorption complex stability increases for all combinations of nanomaterial and solvent. On the other side of the pH range (up to pH 9.5) quinolone molecules adsorbed on graphene show no change in behaviour from neutral pH, while for graphene oxide adsorption complexes become stable in water but desorb in *n*-octanol. This presents the possibility of a latent release of adsorbed quinolones should the nanomaterial flakes encounter an alkaline, low polarity environment.

Sulphonamides adsorb in a stable manner on both nanomaterials in water as well as on graphene oxide in *n*-octanol in acidic conditions, Fig 4. Sulphonamides form more stable adsorption complexes on graphene than graphene oxide in water, which is in accordance with earlier findings on the effect of oxygen containing functional groups on their adsorption on carbon nanomaterials (Wei et al., 2017). The adsorption strength on graphene in water at pH 7 follows the order: sulfasalazine > sulphisoxazole > sulfamethazine ≈ sulfathiazole > sulfaquinoxaline ≈ sulfamerazine > sulfamethoxypyridazine ≈ sulfadimetoxine ≈ sulfabenzamide > sulfamethoxazole > sulfamethizole > sulfadiazine (Table 1 and Table S3 SI). At pH 5, our results display the trend in adsorption stability seen in the previously mentioned research: sulfadimethoxine > sulfamethizole > sulfamethazine > sulfamethoxazole(Wei et al., 2017). Examination of earlier correlations indicate that sulfonamide adsorption is mostly influenced by hydrogen bonding ($r_s(\Delta H$ vs. $\Delta H_{\text{H-bonds}})$= 0.51, $p < .05$) in water and the solvophobic effect. Interestingly, the increase in the strength of the hydrogen bonds upon transfer to *n*-octanol seems to be the result of the strengthening of intramolecular nanomaterial hydrogen bonds upon sulphonamide adsorption, rather than the expected strengthening of intermolecular antibiotic – nanomaterial hydrogen bonds. The effect of the increase in pH on the adsorption of sulphonamides to graphene oxide is destabilizing and leads to desorption above a pH of 8 in *n*-octanol, which is consistent with earlier findings on the effect of pH on the adsorption of sulphonamides to graphene oxide in water(Wu et al., 2016). It is interesting to note that N-acetylated sulphonamides (e.g. N-acetyl-sulfadiazine and N-acetylsulfamethoxazole) exhibit (~14 kJ mol^{-1}) higher binding affinity to graphene in water in comparison to the unmetabolized drug.

β-lactam antibiotics with graphene show the following complex stability rank: cefuroxime > cloxacillin > oxacillin > penicillin G > ampicillin > dicloxacillin > amoxicillin > cephalexin

(Table 1 and Table S3 SI). Again, they adsorb more stably on graphene than on graphene oxide in water, Fig 4. In *n*-octanol adsorption on graphene is unfavourable whereas adsorption complexes on graphene oxide are still stable but less so than in water. This, along with the correlation of Gibbs free energy with the change in solvent available surface area during adsorption (r_s(water) = 0.8, $p < .05$), leads us to conclude that adsorption of β-lactams on graphene is mostly driven by hydrophobic interactions. The sum of hydrogen bond formation enthalpies correlates strongly with the change in adsorption enthalpies from graphene to graphene oxide ($r_s = 0.8$, $p < .05$), when considering the adsorption on graphene oxide in *n*-octanol, while in water the correlation is moderate ($r_s = 0.5$, $p < .05$). This agrees well with the findings of Anchique *et al.* who found that electrostatic interactions (which include hydrogen bonding) comprised the majority of the interaction energy between amoxicillin and graphene oxide (Anchique et al., 2021).

Tetracyclines also form stable adsorption complexes on both nanomaterials in both solvents at neutral pH, Fig 4. This class of antibiotics adsorbs more stably on graphene than graphene oxide in water, with the reverse being true in *n*-octanol. Upon transfer from water to *n*-octanol, adsorption complexes with graphene oxide become more stable, whereas adsorption complexes with graphene become less stable. The solvophobic effect on graphene oxide is also visible as a change from moderate correlation between the adsorption enthalpy and solvent available surface area in water, to no significant correlation in *n*-octanol. The strength of adsorption on graphene was found to follow the order: chlorotetracycline > doxycycline > oxytetracycline > tetracycline (Table 1 and Table S3 SI), which agrees well with previous findings that chlorotetracycline adsorbs onto graphene more strongly than tetracycline The reverse was found to be true for chlorotetracycline and tetracycline on graphene oxide, again corresponding to previous findings. The influence of both increasing pH beyond 8 and

lowering solvent polarity was found to have a destabilizing effect on tetracycline adsorption. This result matches the findings of other researchers who have explored the regeneration of reduced graphene oxide adsorbents with *n*-hexane (Song et al., 2016).

Nitroimidazole antibiotics exhibit the lowest adsorption affinity to graphene compared to other classes of antibiotics, Fig 4. Metronidazole shows greatest adsorption affinity followed by ronidazole, hydroxymetronidazole and dimetridazole (Table 1 and Table S3 SI). This is expected as they are comprised of small neutral molecules with low polarizability, leading to less intense vdW and solvophobic interactions. This class of antibiotics desorbs completely from graphene upon changing the solvent to *n*-octanol and does not adsorb onto graphene oxide in either solvent. The observed behavior on graphene oxide appears to be the result of the inadequate complex stabilization by newly formed hydrogen bonds, which do not compensate well for the weakened vdW and solvophobic interactions as well as for lost π – interactions. Nitroimidazole antibiotics exhibit no difference in the adsorption stability over the examined pH range since they do not change their charge state.

Chloramphenicol and florampheniсol adsorb stably on both CNMs in both solvents, exhibiting greater stability in water on graphene and in *n*-octanol on graphene oxide, as do many antibiotics of other classes, Fig. 4. Trimethoprim, on the other hand, forms more stable adsorption complexes with graphene oxide than graphene in both solvents (Fig. 4), which we propose to be the result of hydrogen bonding as we calculated a sum of hydrogen bond formation enthalpies of over 40 kJ mol^{-1}. This is in agreement with the work of Carrales-Alvarado *et al.* (Carrales-Alvarado et al., 2020) who also found a greater adsorption of trimethoprim on graphene oxide than on graphene (reduced graphene oxide). Lincosamides adsorb in the opposite manner to trimethoprim, forming more stable adsorption complexes

with graphene than graphene oxide in both solvents at neutral pH, Fig. 4. This seems to be the result of both the existence of cation – π interactions when adsorbed on graphene and an increase in the distance of the centers of mass of the antibiotic and nanomaterial molecules upon transition from graphene to graphene oxide. The obtained result is also in line with previous findings that lincomycine adsorbs less strongly to graphene oxide than chloramphenicol in water(Gao et al., 2017).

The data presented show that for conditions expected to be found during wastewater treatment, graphene oxide may require pH adjustments to efficiently adsorb most antibiotic classes and, even then, may not adsorb molecules such as nitroimidazoles. This may be beneficial in cases where the selectivity of adsorption on the nanomaterial is exploited. For such cases of competitive adsorption, the thermodynamic data in table S4 should be useful input for the calculation of competitive adsorption coefficients for the Sheindorf-Rebhun-Sheintuch isotherm.(Sheindorf et al., 1981) In this way, results may contribute to determination of competition coefficient for antibiotics without the need for large amounts of laborious experimental work.

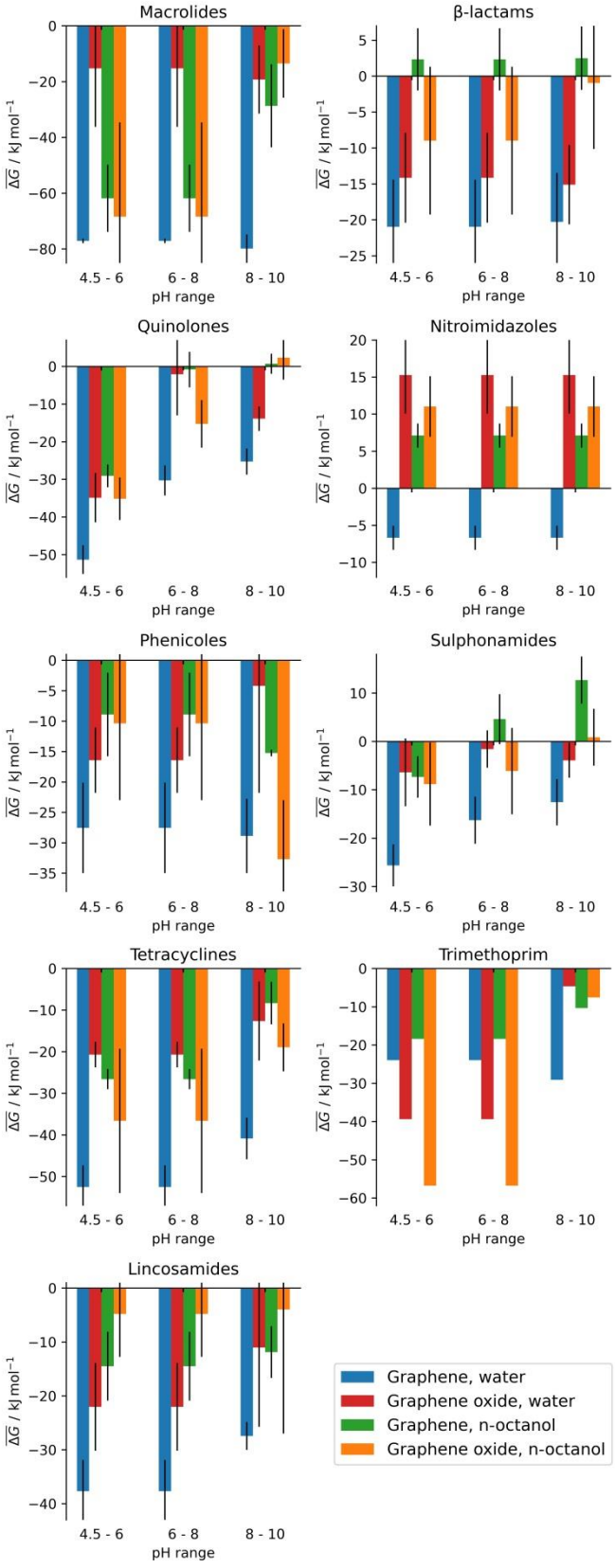
Macrolides
β-lactams
Quinolones
Nitroimidazoles
Phenicoles
Sulphonamides
Tetracyclines
Trimethoprim
Lincosamides
$\overline{\Delta G}$ / kJ mol^{-1}
pH range
4.5 - 6
6 - 8
8 - 10
Graphene, water
Graphene oxide, water
Graphene, n-octanol
Graphene oxide, n-octanol

502

503 Fig. 4. Mean adsorption Δ*G* of antibiotic complexes broken down by solvent, nanomaterial,
504 class and pH range. For specific antibiotic please consult Table S4 in combination with Table
505 S2.

506

507 **Adsorbent regeneration**

508 Three variables were examined here in terms of their effect on nanomaterial regeneration: the
509 solvent, pH range and temperature. Of these the effect of temperature is the clearest,
510 adsorption complexes are less stable at higher temperatures on both nanomaterials, in both
511 solvents and at every pH. Temperatures at which the Gibbs free energy of adsorption is on
512 average zero for each class of antibiotic and broken down by nanomaterial, solvent and pH
513 range are given in Table S7. The data suggest that most antibiotic classes will not desorb from
514 graphene in water at temperatures where water is liquid. On the other hand, in *n*-octanol at
515 100° C, basic conditions, will desorb all antibiotic classes except macrolides which require
516 temperatures in excess of 140° C. From graphene oxide in water, it is possible to desorb all
517 classes of antibiotics at 90° C in alkaline conditions however most classes also desorb at
518 lower temperatures and neutral pH. Desorption temperatures do not follow a clear trend for
519 adsorption complexes on graphene oxide in n-octanol.

520 Less polar solvents may be an interesting option for the regeneration of graphene based
521 adsorbents as adsorption complexes in *n*-octanol were universally less stable than those in
522 water. In addition to reducing solvent polarity, adjusting pH above 8 may lead to even more
523 effective desorption of all antibiotic classes (except phenicoles) from pristine graphene. For
524 the regeneration of graphene oxide based adsorbents, solvent polarity cannot be discussed
525 separately from solution pH as changes of ionic state result in large shifts of the contribution
526 of the solvophobic effect. Most antibiotic classes form less stable adsorption complexes above

527 pH 8 on graphene oxide in water and *n*-octanol. However, macrolides, quinolones,
528 sulphonamides and β-lactam antibiotics in water and phenicoles in *n*-octanol do not lose (or
529 even increase) adsorption strength. Given this variety of responses, graphene oxide adsorbents
530 may require more elaborate regeneration protocols to ensure the adequate desorption
531 antibiotics

532

Conclusions

The adsorption Gibbs free energies of 51 antibiotics on graphene and graphene-based materials provided in this work likely provide the most comprehensive overview of adsorption thermodynamics of antibiotics-carbon nanomaterial complexes. We found that adsorption is guided by various non-covalent interactions that operate simultaneously, including vdW dispersion forces, π interactions, hydrophobic interaction and hydrogen bonding. The magnitude of each particular non-covalent interaction is controlled by the molecular properties of antibiotic and graphene/graphene oxide, as well as the background solution composition. vdW dispersion forces are positively modulated by average molecular polarizability, and negatively modulated by the functionalization of graphene. Although π-π interactions also favour graphene as a sorbent material, more than one aromatic ring on the antibiotic molecule would not additionally contribute to the overall adsorption energy via π-π interactions. Hydrophobic interaction and hydrogen bonding are primarily modulated by solution polarity and pH. Macrolide antibiotics will form the most stable complexes with graphene at environmental pH in water, while antiprotozoal antibiotics will be at the end of the stability ladder. For graphene oxide, complexes formed with trimethoprim antibiotic are the most stable, while antiprotozoal antibiotics form the least stable complexes. At environmental pH, the most efficient removal method for a given set of antibiotics from aquatic environments is the use of graphene as a sorbent material. The subsequent regeneration of the sorbent is best achieved through washing the graphene with slightly basic (pH 8 – 10) non-polar solvents. It appears that the computational pipeline applied in this work provides an efficient tool for elucidating the absorption behaviour of antibiotics onto nanomaterials. Furthermore, we believe that the data presented here will: I) provide guidance for the design of new CNMs as well as tuning of existing ones, II) contribute to the

development of predictive adsorption models, and III) support the elucidation of existing CNM toxicity in terms of their role as antibiotic transport vectors.

Acknowledgements

The authors gratefully acknowledge the computing resources and support provided by The University Computing Centre (SRCE) in Zagreb. Proofreading by Katarina Cetinić (Ruđer Bošković Institute, Zagreb) is gratefully acknowledged. This work was supported by the Croatian Science Foundation project no. IP-2018-01-2298.

Author contributions

Matej Kern: Formal analysis, Methodology, Software, Visualization, Data curation, Writing - original draft, Writing – review & editing.

Sanja Škulj: Formal analysis, Software.

Marko Rožman: Conceptualization, Funding acquisition, Methodology, Supervision, Writing – review & editing.

Conflicts of interest

The authors declare that they have no known competing financial interests or personal relationships that could have appeared to influence the work reported in this paper.

Supplementary information

Full geometries of the presented complexes are available upon request.

1. Supplementary information.pdf

2. Table S4.xlsx

References

Adriaenssens, N., Coenen, S., Versporten, A., Muller, A., Minalu, G., Faes, C., Vankerckhoven, V., Aerts, M., Hens, N., Molenberghs, G., Goossens, H., Metz, S., Fluch, G., Vaerenberg, S., Goossens, M.M., Markova, B., Andrašević, A.T., Kontemeniotis, A., Vlček, J., Frimodt-Møller, N., Jensen, U.S., Rootslane, L., Laius, O., Vuopio-Varkila, J., Lyytikainen, O., Cavalie, P., Kern, W., Giamarellou, H., Antoniadou, A., Ternák, G., Benko, R., Briem, H., Einarsson, O., Cunney, R., Oza, A., Raz, R., Edelstein, H., Folino, P., Seilis, A., Dumpis, U., Valinteliene, R., Bruch, M., Borg, M., Zarb, P., Natsch, S., Kwint, M., Blix, H.S., Hryniewics, W., Olczak-Pienkowska, A., Kravanja, M., Ozorowski, T., Ribeirinho, M., Caldeira, L., Băicuş, A., Popescu, G., Ratchina, S., Kozlov, R., Foltán, V., Čižman, M., Lázaro, E., Campos, J., de Abajo, F., Dohnhammar, U., Zanetti, G., Davey, P., Wickens, H., 2011. European Surveillance of Antimicrobial Consumption (ESAC): Outpatient macrolide, lincosamide and streptogramin (MLS) use in Europe (1997-2009). J. Antimicrob. Chemother. 66, 37–45. https://doi.org/10.1093/jac/dkr456

Ai, Y., Liu, Y., Huo, Y., Zhao, C., Sun, L., Han, B., Cao, X., Wang, X., 2019. Insights into the adsorption mechanism and dynamic behavior of tetracycline antibiotics on reduced graphene oxide (RGO) and graphene oxide (GO) materials. Environ. Sci. Nano 6, 3336–3348. https://doi.org/10.1039/c9en00866g

Alammar, A., Park, S.H., Ibrahim, I., Deepak, A., Holtzl, T., Dumée, L.F., Lim, H.N., Szekely, G., 2020. Architecting neonicotinoid-scavenging nanocomposite hydrogels for environmental remediation. Appl. Mater. Today 21, 100878. https://doi.org/10.1016/j.apmt.2020.100878

Albergamo, V., Blankert, B., Cornelissen, E.R., Hofs, B., Knibbe, W.J., van der Meer, W., de Voogt, P., 2019. Removal of polar organic micropollutants by pilot-scale reverse osmosis drinking water treatment. Water Res. 148, 535–545. https://doi.org/10.1016/j.watres.2018.09.029

Anchique, L., Alcázar, J.J., Ramos-Hernandez, A., Méndez-López, M., Mora, J.R., Rangel, N., Paz, J.L., Márquez, E., 2021. Predicting the Adsorption of Amoxicillin and Ibuprofen on Chitosan and Graphene Oxide Materials: A Density Functional Theory Study.

612 Polymers (Basel). 13, 1620. https://doi.org/10.3390/polym13101620

613 Aquino, A.J.A., Tunega, D., Haberhauer, G., Gerzabek, M.H., Lischka, H., 2002. Solvent
614 effects on hydrogen bonds - A theoretical study. J. Phys. Chem. A 106, 1862–1871.
615 https://doi.org/10.1021/jp013677x

616 Baselga-Cervera, B., Cordoba-Diaz, M., García-Balboa, C., Costas, E., López-Rodas, V.,
617 Cordoba-Diaz, D., 2019. Assessing the effect of high doses of ampicillin on five marine
618 and freshwater phytoplankton species: a biodegradation perspective. J. Appl. Phycol. 31,
619 2999–3010. https://doi.org/10.1007/s10811-019-01823-8

620 Becke, A.D., 1993. Density-functional thermochemistry. III. The role of exact exchange. J.
621 Chem. Phys. 98, 5648–5652. https://doi.org/10.1063/1.464913

622 Boys, S.F., Bernardi, F., 1970. The calculation of small molecular interactions by the
623 differences of separate total energies. Some procedures with reduced errors. Mol. Phys.
624 19, 553–566. https://doi.org/10.1080/00268977000101561

625 Brauer, R., Ruigómez, A., Downey, G., Bate, A., Garcia Rodriguez, L.A., Huerta, C., Gil, M.,
626 Abajo, F., Requena, G., Alvarez, Y., Slattery, J., Groot, M., Souverein, P., Hesse, U.,
627 Rottenkolber, M., Schmiedl, S., Vries, F., Tepie, M.F., Schlienger, R., Smeeth, L.,
628 Douglas, I., Reynolds, R., Klungel, O., 2016. Prevalence of antibiotic use: a comparison
629 across various European health care data sources. Pharmacoepidemiol. Drug Saf. 25, 11–
630 20. https://doi.org/10.1002/pds.3831

631 Carrales-Alvarado, D.H., Rodríguez-Ramos, I., Leyva-Ramos, R., Mendoza-Mendoza, E.,
632 Villela-Martínez, D.E., 2020. Effect of surface area and physical–chemical properties of
633 graphite and graphene-based materials on their adsorption capacity towards
634 metronidazole and trimethoprim antibiotics in aqueous solution. Chem. Eng. J. 402,
635 126155. https://doi.org/10.1016/j.cej.2020.126155

636 Chen, H., Gao, B., Li, H., 2015. Removal of sulfamethoxazole and ciprofloxacin from
637 aqueous solutions by graphene oxide. J. Hazard. Mater. 282, 201–207.
638 https://doi.org/10.1016/j.jhazmat.2014.03.063

639 Daggag, D., Lazare, J., Dinadayalane, T., 2019. Conformation dependence of tyrosine binding
640 on the surface of graphene: Bent prefers over parallel orientation. Appl. Surf. Sci. 483,
641 178–186. https://doi.org/10.1016/j.apsusc.2019.03.181

Dennington, Roy; Keith, Todd A.; Millam, J.M., 2016. GaussView, Version 6.0.

Ersan, G., Apul, O.G., Perreault, F., Karanfil, T., 2017. Adsorption of organic contaminants by graphene nanosheets: A review. Water Res. https://doi.org/10.1016/j.watres.2017.08.010

Frisch, M.J., Trucks, G.W., Schlegel, H.B., Scuseria, G.E., Robb, M. a., Cheeseman, J.R., Scalmani, G., Barone, V., Petersson, G. a., Nakatsuji, H., Li, X., Caricato, M., Marenich, a. V., Bloino, J., Janesko, B.G., Gomperts, R., Mennucci, B., Hratchian, H.P., Ortiz, J. V., Izmaylov, a. F., Sonnenberg, J.L., Williams, Ding, F., Lipparini, F., Egidi, F., Goings, J., Peng, B., Petrone, A., Henderson, T., Ranasinghe, D., Zakrzewski, V.G., Gao, J., Rega, N., Zheng, G., Liang, W., Hada, M., Ehara, M., Toyota, K., Fukuda, R., Hasegawa, J., Ishida, M., Nakajima, T., Honda, Y., Kitao, O., Nakai, H., Vreven, T., Throssell, K., Montgomery Jr., J. a., Peralta, J.E., Ogliaro, F., Bearpark, M.J., Heyd, J.J., Brothers, E.N., Kudin, K.N., Staroverov, V.N., Keith, T. a., Kobayashi, R., Normand, J., Raghavachari, K., Rendell, a. P., Burant, J.C., Iyengar, S.S., Tomasi, J., Cossi, M., Millam, J.M., Klene, M., Adamo, C., Cammi, R., Ochterski, J.W., Martin, R.L., Morokuma, K., Farkas, O., Foresman, J.B., Fox, D.J., 2016. G16_C01.

Gao, Y., Li, Y., Zhang, L., Huang, H., Hu, J., Shah, S.M., Su, X., 2012. Adsorption and removal of tetracycline antibiotics from aqueous solution by graphene oxide. J. Colloid Interface Sci. 368, 540–546. https://doi.org/10.1016/j.jcis.2011.11.015

Gao, Y., Wu, J., Ren, X., Tan, X., Hayat, T., Alsaedi, A., Cheng, C., Chen, C., 2017. Impact of graphene oxide on the antibacterial activity of antibiotics against bacteria. Environ. Sci. Nano 4, 1016–1024. https://doi.org/10.1039/c7en00052a

Gauthier, T.D., 2001. Detecting trends using spearman's rank correlation coefficient. Environ. Forensics 2, 359–362. https://doi.org/10.1080/713848278

Gowtham, S., Scheicher, R.H., Pandey, R., Karna, S.P., Ahuja, R., 2008. First-principles study of physisorption of nucleic acid bases on small-diameter carbon nanotubes. Nanotechnology 19, 125701 (6pp). https://doi.org/10.1088/0957-4484/19/12/125701

Grimme, S., Antony, J., Ehrlich, S., Krieg, H., 2010. A consistent and accurate ab initio parametrization of density functional dispersion correction (DFT-D) for the 94 elements H-Pu. J. Chem. Phys. 132, 154104. https://doi.org/10.1063/1.3382344

672 Hassan, M.N., Rahman, M., Hossain, M.B., Hossain, M.M., Mendes, R., Nowsad, A.A.K.M.,
673 2013. Monitoring the presence of chloramphenicol and nitrofuran metabolites in cultured
674 prawn, shrimp and feed in the Southwest coastal region of Bangladesh. Egypt. J. Aquat.
675 Res. 39, 51–58. https://doi.org/10.1016/j.ejar.2013.04.004

676 He, L., Liu, F. fei, Zhao, M., Qi, Z., Sun, Xuefei, Afzal, M.Z., Sun, Xiaomin, Li, Y., Hao, J.,
677 Wang, S., 2018. Electronic-property dependent interactions between tetracycline and
678 graphene nanomaterials in aqueous solution. J. Environ. Sci. (China) 66, 286–294.
679 https://doi.org/10.1016/j.jes.2017.04.030

680 Iogansen, A. V., 1999. Direct proportionality of the hydrogen bonding energy and the
681 intensification of the stretching ν (XH) vibration in infrared spectra. Spectrochim. Acta -
682 Part A Mol. Biomol. Spectrosc. 55, 1585–1612. https://doi.org/10.1016/S1386-
683 1425(98)00348-5

684 Ivanković, K., Kern, M., Rožman, M., 2021. Modelling of the adsorption of pharmaceutically
685 active compounds on carbon-based nanomaterials. J. Hazard. Mater. 414, 125554.
686 https://doi.org/10.1016/j.jhazmat.2021.125554

687 Jauris, I.M., Matos, C.F., Saucier, C., Lima, E.C., Zarbin, A.J.G., Fagan, S.B., Machado,
688 F.M., Zanella, I., 2016. Adsorption of sodium diclofenac on graphene: A combined
689 experimental and theoretical study. Phys. Chem. Chem. Phys. 18, 1526–1536.
690 https://doi.org/10.1039/c5cp05940b

691 Kanagaraj, K., Alagesan, M., Inoue, Y., Yang, C., 2017. Solvation Effects in Supramolecular
692 Chemistry, Comprehensive Supramolecular Chemistry II. https://doi.org/10.1016/b978-
693 0-12-409547-2.12481-3

694 Kang, J.H., Kim, T., Choi, J., Park, J., Kim, Y.S., Chang, M.S., Jung, H., Park, K.T., Yang,
695 S.J., Park, C.R., 2016. Hidden Second Oxidation Step of Hummers Method. Chem.
696 Mater. 28, 756–764. https://doi.org/10.1021/acs.chemmater.5b03700

697 Kim, D., Hu, S., Tarakeshwar, P., Kim, K.S., Lisy, J.M., 2003. Cation-π interactions: A
698 theoretical investigation of the interaction of metallic and organic cations with alkenes,
699 arenes, and heteroarenes. J. Phys. Chem. A 107, 1228–1238.
700 https://doi.org/10.1021/jp0224214

701 Konkena, B., Vasudevan, S., 2012. Understanding aqueous dispersibility of graphene oxide

and reduced graphene oxide through p K a measurements. J. Phys. Chem. Lett. 3, 867–872. https://doi.org/10.1021/jz300236w

Kovalakova, P., Cizmas, L., McDonald, T.J., Marsalek, B., Feng, M., Sharma, V.K., 2020. Occurrence and toxicity of antibiotics in the aquatic environment: A review. Chemosphere 251, 126351. https://doi.org/10.1016/j.chemosphere.2020.126351

Kümmerer, K., 2009. Antibiotics in the aquatic environment - A review - Part I. Chemosphere 75, 417–434. https://doi.org/10.1016/j.chemosphere.2008.11.086

Lata, S., Vikas, 2021. Concentration-dependent adsorption of organic contaminants by graphene nanosheets: quantum-mechanical models. J. Mol. Model. 27. https://doi.org/10.1007/s00894-021-04686-4

Lin, Y., Xu, S., Li, J., 2013. Fast and highly efficient tetracyclines removal from environmental waters by graphene oxide functionalized magnetic particles. Chem. Eng. J. 225, 679–685. https://doi.org/10.1016/j.cej.2013.03.104

Luo, K., Mu, Y., Wang, P., Liu, X., 2015. Effect of oxidation degree on the synthesis and adsorption property of magnetite/graphene nanocomposites. Appl. Surf. Sci. 359, 188–195. https://doi.org/10.1016/j.apsusc.2015.10.083

Marenich, A. V., Cramer, C.J., Truhlar, D.G., 2009. Universal solvation model based on solute electron density and on a continuum model of the solvent defined by the bulk dielectric constant and atomic surface tensions. J. Phys. Chem. B 113, 6378–6396. https://doi.org/10.1021/jp810292n

Morimoto, N., Kubo, T., Nishina, Y., 2016. Tailoring the oxygen content of graphite and reduced graphene oxide for specific applications. Sci. Rep. 6, 4–11. https://doi.org/10.1038/srep21715

Morimoto, N., Suzuki, H., Takeuchi, Y., Kawaguchi, S., Kunisu, M., Bielawski, C.W., Nishina, Y., 2017. Real-Time, in Situ Monitoring of the Oxidation of Graphite: Lessons Learned. Chem. Mater. 29, 2150–2156. https://doi.org/10.1021/acs.chemmater.6b04807

Pašalić, H., Aquino, A.J.A., Tunega, D., Haberhauer, G., Gerzabek, M.H., Georg, H.C., Moraes, T.F., Coutinho, K., Canuto, S., Lischka, H., 2010. Thermodynamic stability of hydrogen-bonded systems in polar and nonpolar environments. J. Comput. Chem. NA-

NA. https://doi.org/10.1002/jcc.21491

Peng, B., Chen, L., Que, C., Yang, K., Deng, F., Deng, X., Shi, G., Xu, G., Wu, M., 2016. Adsorption of Antibiotics on Graphene and Biochar in Aqueous Solutions Induced by π-π Interactions. Sci. Rep. 6. https://doi.org/10.1038/srep31920

Phoon, B.L., Ong, C.C., Mohamed Saheed, M.S., Show, P.L., Chang, J.S., Ling, T.C., Lam, S.S., Juan, J.C., 2020. Conventional and emerging technologies for removal of antibiotics from wastewater. J. Hazard. Mater. 400, 122961. https://doi.org/10.1016/j.jhazmat.2020.122961

Previšić, A., Vilenica, M., Vučković, N., Petrović, M., Rožman, M., 2021. Aquatic Insects Transfer Pharmaceuticals and Endocrine Disruptors from Aquatic to Terrestrial Ecosystems. Environ. Sci. Technol. 55, 3736–3746. https://doi.org/10.1021/acs.est.0c07609

Rahnama, F., Ashrafi, H., Akhond, M., Absalan, G., 2021. Introducing Ag2O-Ag2CO3/rGO nanoadsorbents for enhancing photocatalytic degradation rate and efficiency of Congo red through surface adsorption. Colloids Surfaces A Physicochem. Eng. Asp. 613, 126068. https://doi.org/10.1016/j.colsurfa.2020.126068

Rizzo, L., Manaia, C., Merlin, C., Schwartz, T., Dagot, C., Ploy, M.C., Michael, I., Fatta-Kassinos, D., 2013. Urban wastewater treatment plants as hotspots for antibiotic resistant bacteria and genes spread into the environment: A review. Sci. Total Environ. 447, 345–360. https://doi.org/10.1016/j.scitotenv.2013.01.032

Rostamian, R., Behnejad, H., 2018. A comprehensive adsorption study and modeling of antibiotics as a pharmaceutical waste by graphene oxide nanosheets. Ecotoxicol. Environ. Saf. https://doi.org/10.1016/j.ecoenv.2017.08.019

Rostamian, R., Behnejad, H., 2016. A comparative adsorption study of sulfamethoxazole onto graphene and graphene oxide nanosheets through equilibrium, kinetic and thermodynamic modeling. Process Saf. Environ. Prot. 102, 20–29. https://doi.org/10.1016/j.psep.2015.12.011

Sedlak, R., Janowski, T., Pitoňák, M., Rezáč, J., Pulay, P., Hobza, P., Pitoňák, M., Řezáč, J., 2013. Accuracy of Quantum Chemical Methods for Large Noncovalent Complexes. J. Chem. Theory Comput. 9, 3364–3374. https://doi.org/10.1021/ct400036b

761 Sheindorf, C., Rebhun, M., Sheintuch, M., 1981. A Freundlich-type multicomponent
762 isotherm. J. Colloid Interface Sci. 79, 136–142. https://doi.org/10.1016/0021-
763 9797(81)90056-4

764 Simon, S., Duran, M., Dannenberg, J.J., 1996. How does basis set superposition error change
765 the potential surfaces for hydrogen-bonded dimers? J. Chem. Phys. 105, 11024–11031.
766 https://doi.org/10.1063/1.472902

767 Song, W., Yang, T., Wang, Xiangxue, Sun, Y., Ai, Y., Sheng, G., Hayat, T., Wang, Xiangke,
768 2016. Experimental and theoretical evidence for competitive interactions of tetracycline
769 and sulfamethazine with reduced graphene oxides. Environ. Sci. Nano 3, 1318–1326.
770 https://doi.org/10.1039/c6en00306k

771 Sophia, A.C., Lima, E.C., Allaudeen, N., Rajan, S., Sophia, A.C., Lima, E.C., Allaudeen, N.,
772 Rajan, S., 2016. Application of graphene based materials for adsorption of
773 pharmaceutical traces from water and wastewater- a review. Desalin. Water Treat. 3994,
774 1–14. https://doi.org/10.1080/19443994.2016.1172989

775 Stephens, P.J., Devlin, F.J., Chabalowski, C.F., Frisch, M.J., 1994. Ab Initio calculation of
776 vibrational absorption and circular dichroism spectra using density functional force
777 fields. J. Phys. Chem. 98, 11623–11627. https://doi.org/10.1021/j100096a001

778 Tang, H., Zhang, S., Huang, T., Cui, F., Xing, B., 2020. pH-Dependent Adsorption of
779 Aromatic Compounds on Graphene Oxide: An Experimental, Molecular Dynamics
780 Simulation and Density Functional Theory Investigation. J. Hazard. Mater. 395, 122680.
781 https://doi.org/10.1016/j.jhazmat.2020.122680

782 Tang, H., Zhao, Y., Shan, S., Yang, X., Liu, D., Cui, F., Xing, B., 2018. Theoretical insight
783 into the adsorption of aromatic compounds on graphene oxide. Environ. Sci. Nano 5,
784 2357–2367. https://doi.org/10.1039/c8en00384j

785 Thakur, K., Kandasubramanian, B., 2019. Graphene and Graphene Oxide-Based Composites
786 for Removal of Organic Pollutants: A Review. J. Chem. Eng. Data.
787 https://doi.org/10.1021/acs.jced.8b01057

788 van der Grinten, E., Pikkemaat, M.G., van den Brandhof, E.J., Stroomberg, G.J., Kraak,
789 M.H.S., 2010. Comparing the sensitivity of algal, cyanobacterial and bacterial bioassays
790 to different groups of antibiotics. Chemosphere 80, 1–6.

https://doi.org/10.1016/j.chemosphere.2010.04.011

Versporten, A., Bolokhovets, G., Ghazaryan, L., Abilova, V., Pyshnik, G., Spasojevic, T., Korinteli, I., Raka, L., Kambaralieva, B., Cizmovic, L., Carp, A., Radonjic, V., Maqsudova, N., Celik, H.D., Payerl-Pal, M., Pedersen, H.B., Sautenkova, N., Goossens, H., 2014. Antibiotic use in eastern Europe: A cross-national database study in coordination with the WHO Regional Office for Europe. Lancet Infect. Dis. 14, 381–387. https://doi.org/10.1016/S1473-3099(14)70071-4

Wang, J., Zhang, P., Liang, B., Liu, Y., Xu, T., Wang, L., Cao, B., Pan, K., 2016. Graphene Oxide as an Effective Barrier on a Porous Nanofibrous Membrane for Water Treatment. ACS Appl. Mater. Interfaces 8, 6211–6218. https://doi.org/10.1021/acsami.5b12723

Wang, Z., Han, M., Li, E., Liu, X., Wei, H., Yang, C., Lu, S., Ning, K., 2020. Distribution of antibiotic resistance genes in an agriculturally disturbed lake in China: Their links with microbial communities, antibiotics, and water quality. J. Hazard. Mater. 393, 122426. https://doi.org/10.1016/j.jhazmat.2020.122426

Wei, J., Sun, W., Pan, W., Yu, X., Sun, G., Jiang, H., 2017. Comparing the effects of different oxygen-containing functional groups on sulfonamides adsorption by carbon nanotubes: Experiments and theoretical calculation. Chem. Eng. J. 312, 167–179. https://doi.org/10.1016/j.cej.2016.11.133

Wu, Y., Xi, B., Hu, G., Wang, D., Li, A., Zhang, W., Lu, L., Ding, H., 2016. Adsorption of tetracycline and sulfonamide antibiotics on amorphous nano-carbon. Desalin. Water Treat. 57, 22682–22694. https://doi.org/10.1080/19443994.2015.1135407

Yadav, N., Lochab, B., 2019. A comparative study of graphene oxide: Hummers, intermediate and improved method. FlatChem. https://doi.org/10.1016/j.flatc.2019.02.001

Yu, F., Li, Y., Han, S., Ma, J., 2016. Adsorptive removal of antibiotics from aqueous solution using carbon materials. Chemosphere 153, 365–385. https://doi.org/10.1016/j.chemosphere.2016.03.083

Zhang, J., Lu, X., Shi, C., Yan, B., Gong, L., Chen, J., Xiang, L., Xu, H., Liu, Q., Zeng, H., 2019. Unraveling the molecular interaction mechanism between graphene oxide and aromatic organic compounds with implications on wastewater treatment. Chem. Eng. J. 358, 842–849. https://doi.org/10.1016/j.cej.2018.10.064

821 Zhang, X., Shen, J., Zhuo, N., Tian, Z., Xu, P., Yang, Z., Yang, W., 2016. Interactions
822 between Antibiotics and Graphene-Based Materials in Water: A Comparative
823 Experimental and Theoretical Investigation. ACS Appl. Mater. Interfaces 8, 24273–
824 24280. https://doi.org/10.1021/acsami.6b09377

825 Zhou, X., Zeng, Z., Zeng, G., Lai, C., Xiao, R., Liu, S., Huang, D., Qin, L., Liu, X., Li, B., Yi,
826 H., Fu, Y., Li, L., Wang, Z., 2020. Persulfate activation by swine bone char-derived
827 hierarchical porous carbon: Multiple mechanism system for organic pollutant
828 degradation in aqueous media. Chem. Eng. J. 383, 123091.
829 https://doi.org/10.1016/j.cej.2019.123091

830 Zhu, X., Tsang, D.C.W., Chen, F., Li, S., Yang, X., 2015. Ciprofloxacin adsorption on
831 graphene and granular activated carbon: Kinetics, isotherms, and effects of solution
832 chemistry. Environ. Technol. (United Kingdom) 36, 3094–3102.
833 https://doi.org/10.1080/09593330.2015.1054316

834